Development of an Ultra-Short 2.0 Micron Seed Pulse

A Senior Thesis

Presented in partial fulfillment of the Requirements for graduation with distinction in Physics

in the undergraduate colleges of The Ohio State University

by

Christoph A. Roedig

The Ohio State University

June 2006

Project Advisor: Professor Louis DiMauro, Department of Physics

Abstract:

One of the exciting advances in ultra-fast optics is the development of a new amplifier architecture known as Optical Parametric Chirped Pulse Amplification (OPCPA). This new mode of amplifying light pulses is unique since it makes amplification of light pulses at arbitrary frequencies possible. In the laboratory of Dr. Louis DiMauro a project is underway to develop an OPCPA based laser system that operates at a wavelength of 2.0 microns, which lies in the mid-infrared part of the electromagnetic spectrum. The system will be the first operational OPCPA at this wavelength. An important part of this project is the development of an ultra-short seed pulse at this wavelength. This pulse will provide the signal, which will be amplified by the OPCPA system. Since no active gain medium exists, that can actively produce ultra short pulses at 2.0 microns; non-linear optics must be employed to convert light from a more conventional and well developed ultra-short laser source. Titanium doped sapphire is a lasing medium that supports large a spectral bandwidth. Titanium sapphire (Ti:S) allows for the generation of extremely short pulses ranging down to 6 femtoseconds (6.0×10^{-15} seconds). The difference in frequencies at the ends of the spectrum of a short Ti:S pulse can lie in the mid-infrared. By using a material with a sufficient nonlinear optical response it is possible to couple the components in the spectral ends of the pulse to produce an ultrashort mid-infrared pulse. We report progress in developing a Ti:S laser oscillator operating at a bandwidth of 70nm and computational simulations for the generation of light pulses at 4.0 microns. This development will aid in assessing the feasibility of utilizing this technique for the generation of the OPCPA seed pulse.

Acknowledgements:

I would like to thank my research advisor, Dr. Louis DiMauro, for his help and guidance and good advice as well as access to excellent laboratory facilities and resources throughout my two years of undergraduate research experience. The opportunities and experience made possible by Dr. DiMauro have allowed me to learn a great deal about science and my self as a scientist.

I would also like to thank Phillip Colosimo, Anne Marie March, Cosmin Blaga, Dr. Kevin Schultz as well as all other graduate students and post doctorates of the DiMauro group for sharing their expert technical knowledge and skills and their patience in answering question and helping me solve problems. Working with the DiMauro group has truly been a motivating experience.

I would like to express my great appreciation to my family especially my parents Reinhold and Virginia Roedig as well as my grandmother Hazel Oshen. Their continuing motivation and support throughout my undergraduate career have allowed me allowed me to achieve any goals I have set for myself and will continue to have a significant impact on my career.

Vita

July 27th, 1982……Born – Hirschau, Germany

September 2001 – June 2006…….Undergraduate Student,

The Ohio State University, Columbus, Ohio

Field Of Study

Major Field: Physics

Table of Contents

List of Figures

List of Equations

Introduction

The field of ultra-fast optics has made vast advances in the last 15 years. Scientists have been able to achieve the generation of light pulses as short as 4 to 6 femto seconds (1fs = 10^{-15} seconds) and peak powers beyond the terawatt regime. Electric fields at these time and energy scales allow the study of strongly perturbative interactions with atoms. These interactions include multi photon ionization, high harmonic generation and the generation of extreme ultraviolet and soft x-ray light pulses which can have durations measured in atto-seconds (1as = 10^{-18} seconds). While pulses in the femto second regime allow study of very fast events such as biological chemical or molecular processes. Pulses in the attosecond regime approach the timescales of more fundamental atomic processes.

Advances based on Titanium Saphire (Ti:S) ultra fast laser technology have pushed the duration of pulses down to that of a few cycles of the electric field at that frequency. Ti:S lasers primarily produce light at 800nm (near infrared) the optical period at this wavelength is approximately 2.7fs. This is the lower limit in pulse duration for this wavelength, since a shorter pulse would no longer contain a full period of the field and thereby would not satisfy Maxwell's equations for a propagating wave [1]. This demonstrates that the possibilities of producing short and intense pulses in the 800nm region have nearly reached their physical limits. However this is only the case for the Ti:S based systems. Even though the laser based production of short pulses from other materials is possible. Ti:S is unique in that it is the only material known to support the bandwidth for lasing in few cycle pulses.

There is much interest in producing ultra short pulses with high intensities at wavelengths other than those possible with Ti:S based systems. Some examples are the cases mulit photon ionization and high harmonic generation. It is known that the rate for these

processes is much higher when driven by longer wavelength fields, such as pulse in the mid infrared region of the electromagnetic spectrum (1.5 to 5.0 microns) [3]. Current approaches of generating short pulses in the mid-infrared involve using nonlinear optics for frequency conversion of an amplified Ti:S laser pulses. These systems rely on difference frequency generation where pulses from two laser systems at different frequencies are mixed to produce the desired frequency, or optical parametric amplification systems where fluorescence arising from the Ti:S pulses is mixed with the same pulse to produce the desired frequency. These schemes are vastly inefficient and require a full Ti:S based laser amplifier system and some times a second laser system. The conversion of light from an 800nm pulse to a 2 micron pulse is at best 20% efficient, this inefficiency is added to the 20% conversion efficiency of the Ti:S laser system itself. In addition to the conversion inefficiency of the mixing process, the possibility of damaging the mixing medium limits the achievable intensity of the generated light.

A way to increase the efficiency and reliability of the generation of mid-infrared pulse is a scheme where the mid-infrared pulse is generated at a very low intensity and then amplified. A possible implementation of this idea is an amplifier architecture known as Optical Parametric Chirped Pulse Amplification (OPCPA). An OPCPA system combines the benefits of direct amplification at any wavelength with the benefits of chirped pulse amplification. Chirped pulse amplification is used in Ti:S based amplifier systems [9]. A CPA system uses a dispersive apparatus (a pair of gratings, prisms or chirped mirrors) to stretch the pulse in time before amplification and recompresses the pulse to its original short duration after amplification. It allows for higher gain since the peak intensity is lowered during amplification to prevent damage to the amplifying medium and associated optics.

Lowering the intensity also reduces parasitic and distorting nonlinear effects, allowing for a more controllable amplifier [2]. Since the OPCPA system does not rely stimulated emission for amplification, it is not subject to the bandwidth restrictions that limit the performance conventional laser amplifiers.

An important consideration in developing the OPCPA system is generation of a seed pulse that will be amplified by the system. The progress described in this work is towards investigating the use of a Ti:S based laser oscillator and non-linear optics to generate an ultra-short seed pulse at a wavelength of 2.0 microns. The large bandwidth associated with a short pulse at 800nm carries frequencies that that have enough separation to have a frequency difference equivalent to mid-infrared frequencies. A suitable nonlinear medium can couple these frequency components such that it generates pulse at the difference of the frequencies. Thus it is possible to convert ultra short pulses from a titanium sapphire based oscillator to ultra short pulses in the mid-infrared spectral region to seed an OPCPA system at that wavelength. The two main components of this research is the construction of a modelocked Ti:S oscillator operating at a bandwidth of 100nm and the conversion of the 800nm oscillator pulses to 4.0 micron pulses by difference frequency mixing of the spectral wings in periodically poled lithium niobate. Studying the conversion process to 4.0 microns will provide insight into exploiting this technique for the generation of ultra short 2.0 micron pulses. I am reporting progress in the construction of the oscillator, as well as preliminary simulations of the conversion process in the periodically poled lithium niobate crystal.

1. Ultra Short Pulses from a Modelocked Ti:S Oscillator

1.1 Short Light Pulses

The time scales approached in this field of research are on the order of femto-seconds (10^{-15} seconds). These short time scales approach the duration of the optical cycles themselves. As a result of this fundamental limitations and restrictions that apply to waves and pulses become significant. The duration of light pulses is restricted a time bandwidth product relation.

$$\Delta t \, \Delta f \gtrsim 0.44 \qquad \textit{eq. 1.11}$$

Eq1.11 time bandwidth product relation for gaussian pulses

Where △f is the bandwidth in frequency and △t is the duration in time. The relation in equation 1.11 states that a short light pulse must contain a large bandwidth in frequency and conversely, a light wave with a precisely defined frequency must have a long duration. The origin of this relationship is mathematically similar to the origin of Heisenberg's uncertainty principle, which relates uncertainties in a particles momentum and position. This can easily be illustrated with examples from acoustics. For example, when comparing the sound emitted from striking a tuning fork to the sound emitted when hitting a wood block.

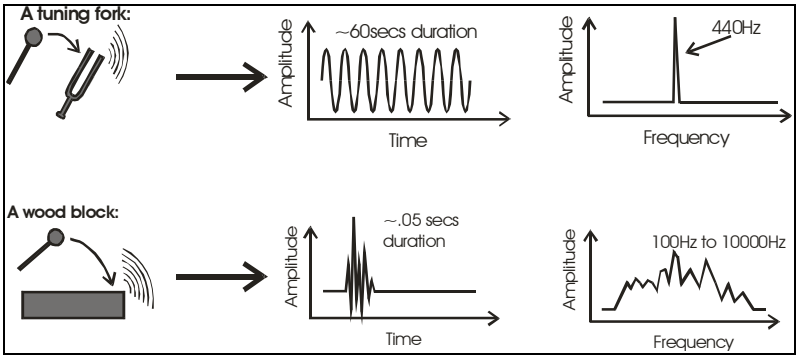

Fig1.11 Two time bandwidth product limiting cases in acoustics

The tuning fork rings precisely defined at 440Hz for several minutes. The wood block sounds with a click, which lasts for a fraction of a second, but emits a wide variety of frequencies across the audible spectrum. Short pulses arise from the superposition and constructive interference of several waves at different frequencies.

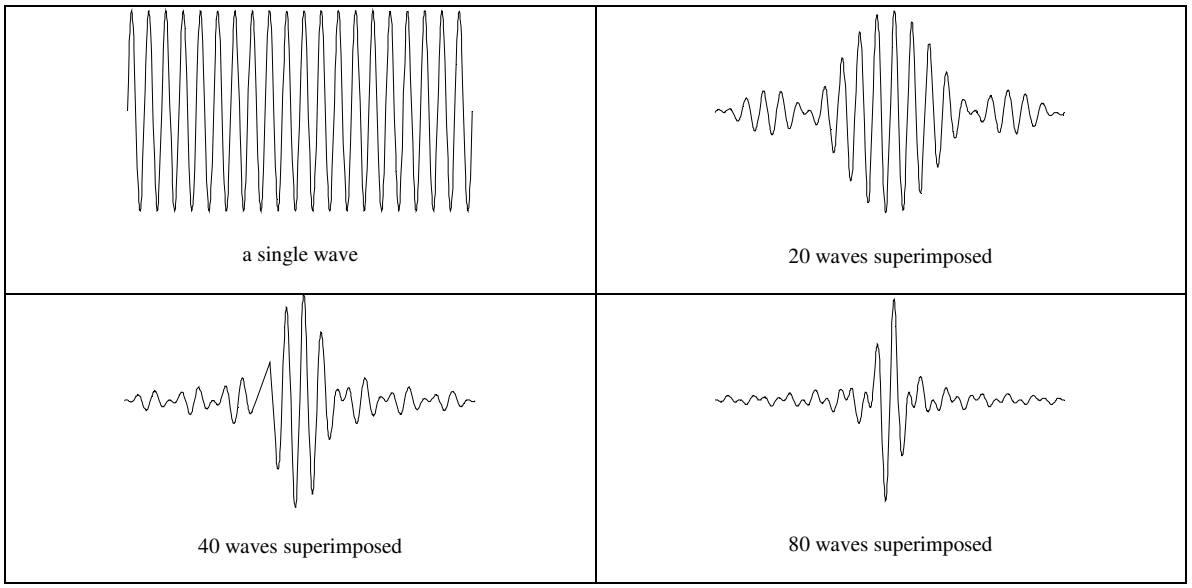

Fig. 1.12 construction of pulses from several waves

Figure 1.12 shows the construction of a pulse from the superposition of several waves. As more waves are added the pulse becomes shorter in duration. An important assumption made for the pulses in this drawing, is that all of their constituent waves have a well-defined, purely linear phase relationship. The phase relationship between the waves is also known as spectral phase. Should the spectral phase be random throughout the spectrum, the result will simply be random noise. The frequency dependant phase of a pulse can be expanded in powers of frequency [2].

$$\phi(\omega) = \phi(\omega_0) + (\omega_0 - \omega)\left.\frac{\delta\phi(\omega)}{\delta\omega}\right|_{\omega=\omega_0} + \frac{(\omega_0 - \omega)^2}{2}\left.\frac{\delta^2\phi(\omega)}{\delta\omega^2}\right|_{\omega=\omega_0} + \ldots + \frac{(\omega_0 - \omega)^n}{n!}\left.\frac{\delta^n\phi(\omega)}{\delta\omega^n}\right|_{\omega=\omega_0}$$

eq. 1.12 Taylor expansion of the frequency dependant phase

The first term is the absolute phase of the carrier field inside the pulse envelope. The second term is known as group delay and describes an arbitrary time shift of the pulse. The

third term is the quadratic phase, quadratic phase can be introduced by a medium that has properties of group velocity dispersion (GVD). This term and higher order terms have a significant impact on the duration of a pulse. A non-zero group velocity dispersion will result in a time dependant frequency sweep throughout the pulse. This is also known as chirp. Higher order terms of the phase such as third order dispersion and higher orders of dispersion also cause stretching of the pulse. In the experimental setting second and third order phase terms have the most impact and are most carefully considered. A pulse with zero quadratic phase and zero higher order phase terms is known to be transform limited, in this condition the pulse will have the shortest possible duration allowed by its bandwidth.

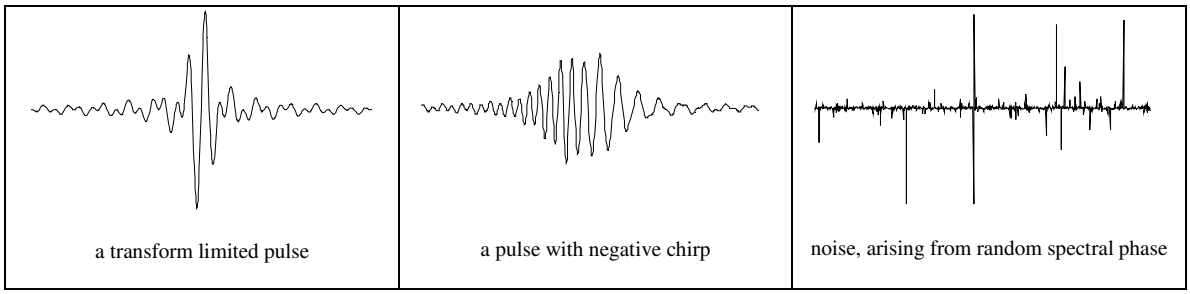

Fig. 1.13 Effects of spectral phase on pulses

Figure 1.13 shows three examples of pulses with the same bandwidth but different spectral conditions. The transform-limited pulse subtends about two cycles in duration. The second pulse is negatively chirped, the frequency decreases in time. It has a much longer duration of about 10 cycles. The last pulse is simply noise, caused by a completely random spectral phase function.

Thus the challenge in generating ultra short light pulses is producing coherent light across a wide range of frequencies and maintaining the transform limited phase relationship. This is achieved with the modelocked oscillator.

1.2 The Modelocked Laser Oscillator

The properties making pulsed operation from a modelocked laser possible is the support of several waves (modes) lasing across a large frequency spectrum and the ability to maintain a spectral phase relationship that allows short pulses.

The resonating system of a laser consists of a cavity that allows modes to resonate and a gain medium that drives energy into the cavity modes.

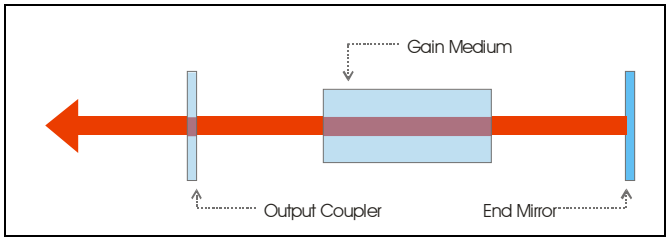

Fig 1.21 A simple laser cavity with gain medium

The gain medium must have an atomic structure such that a preference for stimulated light emission can be introduced. This requires a constant population inversion in the atomic energy levels and a cavity that promotes stimulated emission.

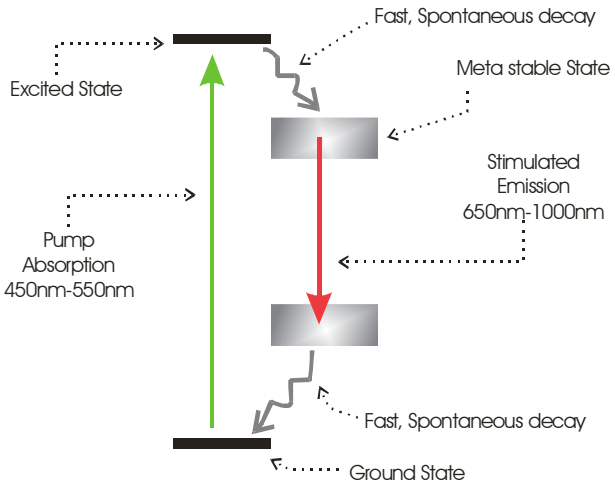

Fig 1.22 Ti:S Laser energy level schematic

Stimulated emission in a titanium sapphire laser occurs in a atomic system with four energy levels. The energy is initially transferred to the system with another laser operating in the absorption spectrum of the material. This is known as pumping. The atoms in the focus of the pump beam are brought into an exited state. From the excited state they quickly decay to a meta-stable state that has a much longer lifetime than the excited state. The long lifetime of the meta-stable state causes the population inversion. Population inversion describes the situation where the majority of the atoms in the gain medium are in the meta-stable state. In this state the atoms can emit light spontaneously or by stimulated emission, should a photon of the frequency corresponding to the transition be present. Initially, light will be emitted spontaneously in all directions, some of this light will be directed back to the gain medium by the end mirror and output coupler. The returning light triggers stimulated emission of more light from the atoms. The photons emitted by stimulated emission will have the same frequency and phase as the photons that triggered the emission. The mirrors that define the ends of the cavity ensure that the majority of light generated by the gain medium is a result of stimulated emission. The distance between the mirrors defines the set of frequencies that the laser operate on. The cavity forms a resonating system that supports standing electromagnetic waves. Each of these waves (modes) must be multiple of the fundamental cavity mode. The fundamental mode frequency is defined by the speed of light and the length of the cavity. It is the inverse of the round trip time for light between the end mirrors. In a Ti:S oscillator the fundamental frequency is usually 80MHz, which lies in the radio frequency spectrum. Ti:S supports much higher multiples of this fundamental frequency that lie in the near infrared to visible

light spectrum. Stimulated emission in Ti:S can span across a broad band of frequencies. This broad band corresponds to over one million different cavity modes.

A laser usually operates at one single cavity mode, closest in frequency to the peak of the emission spectrum. However, it is possible to force the laser (using filters etc.) to operate at other single frequencies in the emission spectrum. A laser oscillator is designed such that several modes across the emission spectrum are brought to lase at once. The modes will then interfere to construct a pulse. This pulse will propagate between the end mirrors of the cavity, part of it exiting at each round trip, through a partially transmissive end mirror (output coupler). Each pass through the crystal amplifies away any energy loss since the last pass. Since the pulse is composed of several waves with discretely spaced frequency, the frequency spectrum of a pulse will be a series of discretely spaced peaks.

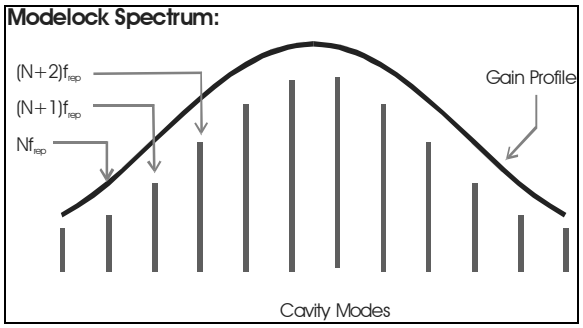

Fig 1.23 The output spectrum of a modelocked oscillator

The peaks will be evenly spaced in frequency by the fundamental frequency, which is also the rate at which pulses emerges from the output coupler. The intensity of each peak is governed by the emission profile of the gain medium. This profile can be approximated as a gaussian function. Figure 1.24 illustrates a discrete modelocked frequency spectrum. The spacing in the drawing however is widely exaggerated, a real Ti:S oscillator has on the order of one million discrete cavity modes in its spectrum. Most common spectrometers cannot resolve the fine spacing between an oscillator's frequency modes.

1.3 Modelocked Oscillator Design and Tuning:

The oscillator built for this experiment is based on a design developed by the Kapteyn – Murnane group at the Washnington State University in 1993 [5], the design plans of which were published from the university of Michigan in 1996 [4]. The design was slightly modified for this experiement. The Oscillator is pumped with a more efficient and reliable frequency doubled Nd:YVO_4 Laser (SpectraPhysics Millenia) at 532nm. The original design was pumped with an Argon-Ion Laser at 488nm. Two folding mirrors were added to the design to allow a more compact layout and the ability to mount the system on an optical bread board, such that it can be moved without disassembly.

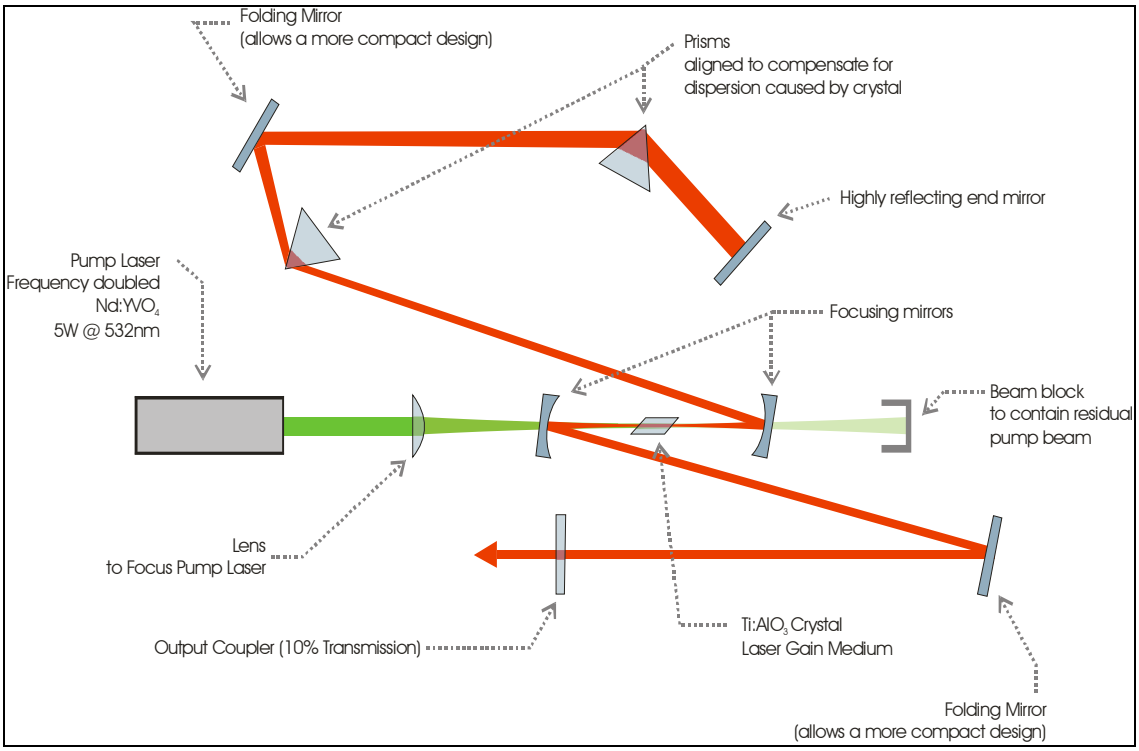

Fig 1.31 Optical component layout of the Titanium Sapphire Based Laser Oscillator

Figure 1.31 shows a schematic of the layout of the oscillator. The pump beam in the actual device is steered in from the top of drawing and brought to the correct height with a periscope. The periscope also rotates the pump beam polarization by 90 degrees to match that of the cavity beam. The output beam is steered back towards the right side of the drawing and lowered with a periscope to match the typical height of measurement equipment and the rest of the experiment. Not shown is a photodiode to display the cavity beam profile in time. This is essential since it provides useful information concerning the repetition rate of the laser, as well as a qualitative indicator of pulsed operation.

The important factors in the design of a modelocked oscillator are dispersion control, bandwidth and stability. Dispersion control refers to the ability of the system to maintain the phase relationship of the modes that corresponds to the shortest possible pulse. Since many of the components especially the Ti:S crystal have a wavelength dependant index of refraction, the different frequency components of the pulse will experience varying amounts of delay. The phase accumulated in a material as a function of frequency ω can be expressed as,

$$\phi(\omega) = \frac{\omega n l_m}{c} \qquad \textit{Eq. 1.31}$$

where n is the index of refraction at ω, l_m is the length of the material and c is the speed of light [1]. The resulting group velocity dispersion derived from this phase is,

$$\frac{d^2\phi}{d\omega^2} = \frac{\lambda^3 l_m}{2\pi c^2}\frac{d^2 n}{d\lambda^2} \qquad \textit{Eq. 1.32}$$

λ in this case the central wavelength of the pulse passing through the material and $\frac{d^2 n}{d\lambda^2}$ is the second derivative (curvature) of the frequency dependent refractive index curve [1]. $\frac{d^2 n}{d\lambda^2}$ is usually positive in materials transparent to visible light. Titanium sapphire thus

produces a positive GVD. A Ti:S also introduces significant third order dispersion. The second and third order dispersion results in an effective stretching of the pulse with each pass through the crystal. If left uncompensated, the pulse would essentially decompose itself after a few passes through the crystal. In order to maintain operation with the shortest possible pulses, a device must be inserted in the cavity that compensates for the dispersion introduced by the crystal with each pass of the pulse. In the design implemented for this experiment a pair of prisms is used in an arrangement known as a prism compressor.

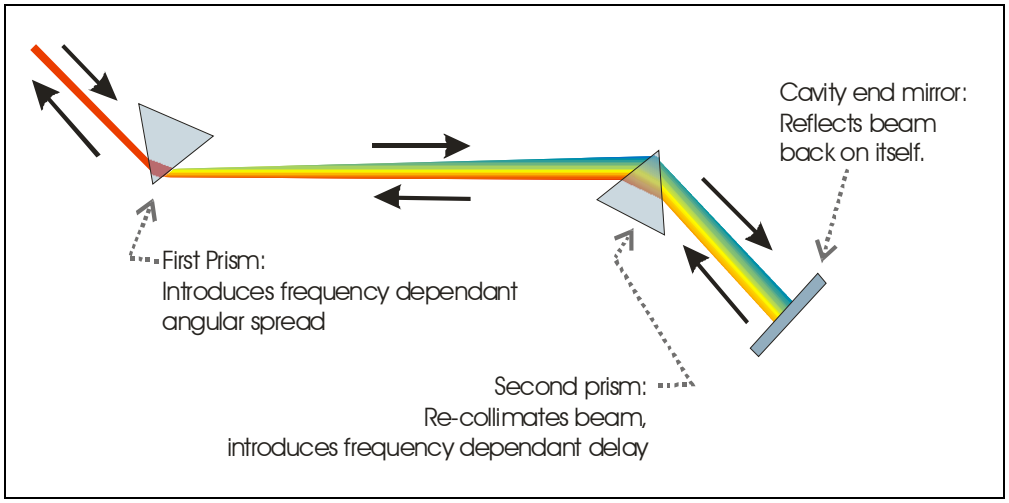

Fig 1.32 Prism Based Delay Line (colors are exaggerated for demonstrational purposes)

The prism pair introduces a negative GVD by spatially separating the modes of the pulse and passing them through varying amount of glass. In this case the higher frequency ("blue") components are passed through less glass than their lower frequency ("red") counterparts. As a result the blue components will leave the prism compressor first followed by the red components.

The frequency dependant phase introduced by a prim pair is,

$$\phi(\omega) = \frac{2\omega l_p}{c}\cos\left(\theta^{blue} - \theta\right) \qquad \textit{eq. 1.33}$$

where l_p is the apex to apex separation between the prism. θ^{blue} is the exit angle of the highest frequency mode from the first prism and $\Theta(\omega)$ is the frequency dependent exit angle from the same prism [2].

The frequency dependant exit angle $\Theta(\omega)$ is,

$$\theta(\omega) = \text{ArcSin}\left[n(\omega)\,\text{Sin}\left[\alpha - \text{ArcSin}\left(\frac{\text{Sin}(\theta_i)}{n(\omega)}\right)\right]\right] \quad \textit{eq. 1.34}$$

where θ_i is incident angle on the first prism, α is the apex angle of the prisms and $n(\omega)$ is the frequency dependant index of refraction of the prism material [2]. The apex and incident angles are selected such that the incident beam experiences the least possible surface reflection from the prism face and the transmitted beam is a minimum deviation after the prisms. The group velocity dispersion introduced by the prism pair is derived from Eq.5,

$$\frac{d^2\phi}{d\omega^2} = \frac{l_p}{c}\left((4\theta'[\omega] + \theta''[\omega]2\omega)\,\text{Sin}\left[\theta^{blue} - \theta[\omega]\right] - \theta'[\omega]^2 2\omega\,\text{Cos}\left[\theta^{blue} - \theta[\omega]\right]\right) \quad \textit{eq.1.35}$$

Under the approximation that the angle difference $\theta^{blue} - \theta[\omega]$ is close to zero for all modes of the oscillator, the sine and cosine terms reduce to zero and one respectively and the expression simplifies to

$$\frac{d^2\phi}{d\omega^2} \cong -\frac{l_p}{c}\theta'[\omega]^2 2\omega \quad \textit{eq. 1.36}$$

where $\theta'[\omega]$ is the change in exit angle with respect to frequency. This expression for GVD is always negative and directly proportional the prism separation. The amount of negative dispersion can be controlled by changing the separation between the prisms, but also by varying the insertion of the prisms into the beam. By increasing the insertion of the prisms, more positive GVD (described by eq. 1.36) and TOD, arising from the prism material can be introduced. Thus most of the positive dispersion arising from the crystal can be removed

by tuning the positions of the prisms. In this design, the approximate prism separations, angles and the prism material were selected by calculation in the work of the Kapteyne - Murnane group. The best performance is achieved at a separation of 58.8cm [4]. Fine-tuning of the insertion and separation must be determined empirically by examining the oscillator performance and making careful adjustments.

The bandwidth supported by the laser is critical in achieving short pulses. It is also critical for the purpose of this experiment in providing enough energy to the spectral components that have the necessary frequency difference to produce mid-infrared pulses. Every optic in the oscillator cavity must be highly reflective (>99%) across the full bandwidth. High bandwidth dielectric mirrors were chosen for all reflective optics. This type of mirror is coated for specific incident angles. Most of the mirrors in the cavity have incidence angles close to 0 degrees and were appropriately equipped with 0 degree dielectric mirrors. The folding mirrors have rather large incidence angles, as a result the design had to be tested with different types of mirrors, since a 45 degree mirror may perform better in certain situations. The optimal results were achieved with 0 degree mirrors. Another factor affecting bandwidth is alignment of the focus in the crystal. The focus position can vary slightly with frequency. This imposes very close tolerances on the alignment to ensure the most efficient focusing. The focusing is also determined empirically by optimizing output power and bandwidth.

Since the stimulated emission process naturally prefers a single frequency, a typical laser will be stable at single mode operation. In order to make modelocked operation possible, the oscillator must be designed such that pulses are amplified with preference over continuous waves. This stability is accomplished using nonlinear optical effects.

The index of refraction of material has an additional intensity dependant term,

$$n \cong n_0 + n_1 I \quad \text{eq. 1.37}$$

where **I** is the intensity of the incident light and n_1 governs the strength of the second term [6]. This term becomes significant at the intensities of the pulses in the cavity, which are orders of magnitude higher than the continuous intensity. Since the intensity of the beam is not spatially uniform but rather higher towards the center and decreasing radially outwards, the beam will be subject to a spatially varying index of refraction, induced by its intensity. This spatially varying index causes the portion of the wave front, towards the center of the beam, to experience a greater delay. This effectively adds curvature to the wave fronts, which is equivalent to focusing. Since the pulses have peak powers of on the order of hundreds of kilowatts and the continuous waves have average powers of less than one watt, the more intense pulsed light will focus itself in the Ti:S crystal, while the CW light remains unaffected. Self-focusing is small compared to the focusing already caused by the curved mirrors, but it does change the position of the focus enough to affect the operation of the laser. The effective focal length of the curved focusing mirrors is reduced by self-focusing. The oscillator is tuned to more stable modelocked operation by changing the positions of the focusing mirrors to account for the shorter focal length caused by self focusing. The modified focusing arrangement is no longer optimized for CW operation. As a result the system will be unstable and inefficient in CW operation and will prefer the modelocked operation.

When the oscillator is first supplied with energy it operates in an unstable and inefficient CW mode. Modelocking must be started artificially by introducing a disturbance to the operation of the laser. This disturbance causes additional modes to briefly start

lasing. At some point during the disturbance some of the modes will randomly construct a pulse. Once a pulse is created, it will dominate in efficiency and the energy of the gain medium will be transferred into the pulse, thus suppressing the CW operation. In most systems, adding mechanical vibrations to one of the optics causes the necessary disturbance. In this design, the noise is most efficiently introduced by briefly moving the second prism by hand. If the laser is optimally tuned, tapping a tool on the optical table near the oscillator will initiate modelocking.

Additional considerations for stability outside of optical alignment are an enclosure to limited air currents and dust in the beam path and closed loop cooling of the crystal. Air currents especially in areas where the beam is focused can distort the spatial profile of the beam and make the focus unstable. For prolonged stable operation, the laser system must be fully enclosed. A buildup of heat can cause the index of refraction of the crystal to change, which can disturb the dispersion tuning of the laser. This sets the requirement that the crystal is constantly cooled during operation to ensure that any heat is efficiently removed, such that the temperature remains stable.

1.4 Results:

Construction, alignment and tuning of the oscillator proved to be a challenging and time consuming task. However, satisfactory results towards the generation of mid-infrared pulses were achieved.

The bandwidth of the oscillator was measured at 65nm. This bandwidth provides enough energy in the spectral wings of the pulse to produce the 4.0 micron mid IR pulses for the experiment. The spectrum was measured with an ocean optics USB2000 ccd array

spectrometer. Output power at this bandwidth was measured at 380mW. The central wavelength of the laser was measured at 773nm.

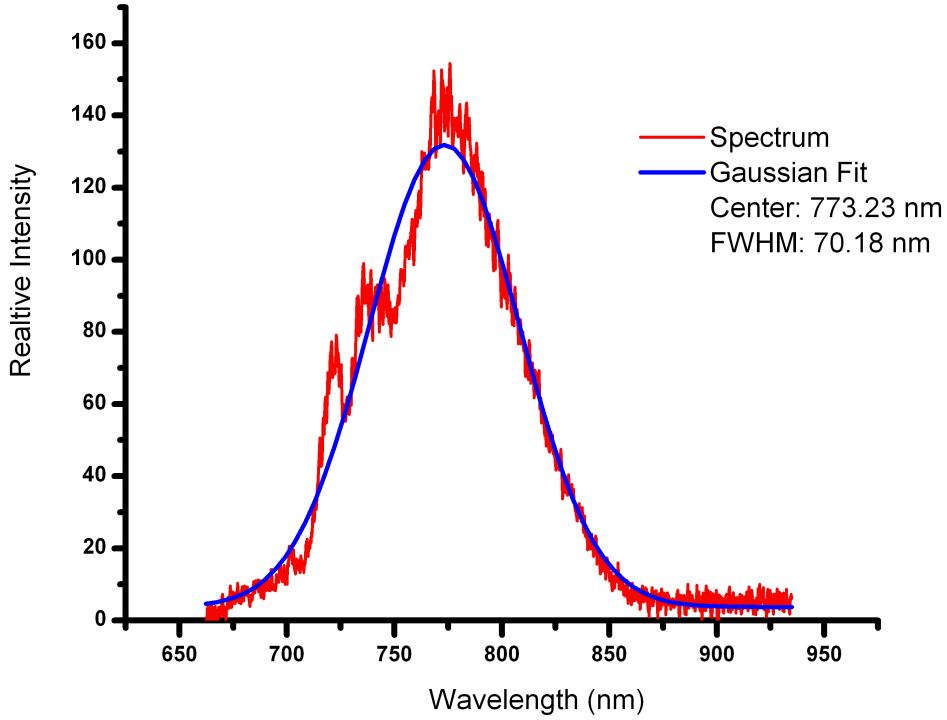

Fig 1.41 Power spectrum of the Modelocked Oscillator

At this bandwidth, the theoretical transform limited duration of the pulse is 13.5fs. However the operation at this bandwidth was not optimal. As seen in the spectrum in Fig 1.41, the blue end (left side of the curve) of the spectrum has some distortions and does not follow the gaussian fit very well. This distortion may arise from alignment problems in the prism compressor. The spreading beam incident on the second prism is partially clipping the tip of the prism. Therefore much of the possible bandwidth in the higher frequency range is sacrificed. Probing the light that is missing the prism confirmed this. The light missing the second prism is centered at about 720nm and extends as low as 650nm. Moving the prism into the beam into the prism to add this light to the bandwidth destabilizes the system, since too much positive dispersion is added.

Measuring the bandwidth of the laser does not provide sufficient information on the properties of the pulses. Measurements of the spectral phase and resulting pulse duration must be conducted. This proves to be a very complicated undertaking.

Since the frequencies of the pulses are on the order of hundreds of terahertz (usually ~3.7 10^{14} Hz) and the durations are on the order of femtoseconds (usually ~$1.0*10^{-14}$s). Direct measurements of the temporal envelope much less the electric field are impossible since even the fastest photodiodes can resolve durations as short as a few nanoseconds ($1.0*10^{-9}$) at best. The electric field must therefore be "reconstructed" analytically from interference effects of the pulse with itself. The device used for measurements in this experiment is named S.P.I.D.E.R. , which stands for Spectral Phase Interferometry for Direct Electric Field reconstruction. The SPIDER allows for the calculation of the second and higher order spectral phase components of the pulse [8]. This allows for the reconstruction of the time profile of the pulse. A full description of this measurement technique is given in the paper, "Spectral phase interferometry for direct electric-field reconstruction of ultrashort optical pulses," by Ian Walmsley [8].

SPIDER measurements on the oscillator operating at 65nm bandwidth were difficult since the spatial profile of the beam was severely distorted, the measurements also reveled a distorted time profile.

The oscillator was tuned to more conservative parameters that limit the beam clipping from the second prism and improve the spatial profile of the beam. In this mode of operation the oscillator produced 50nm of bandwidth.

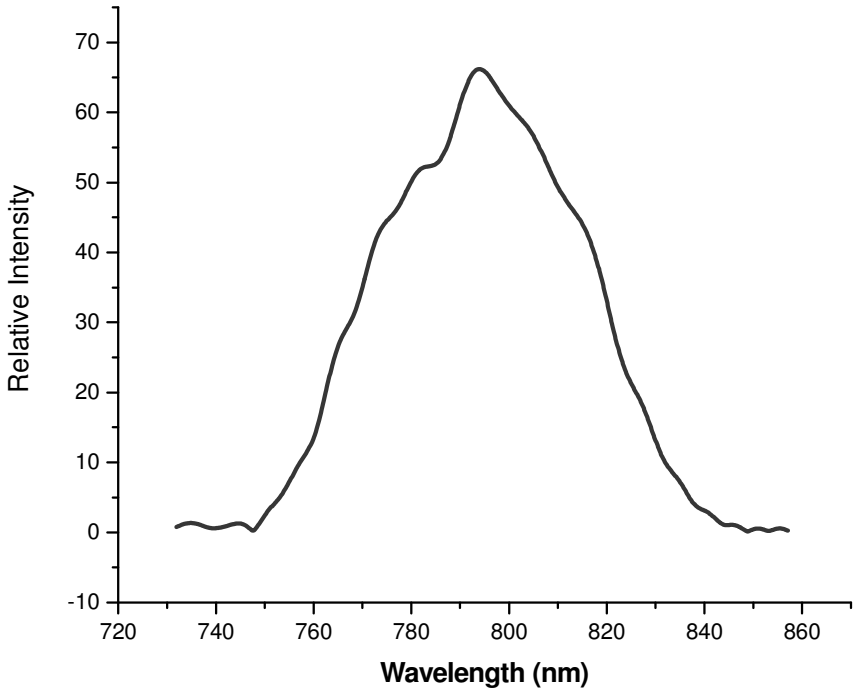

Fig 1.42 Pulse spectrum extracted by the spider

Figure 1.42 shows the bandwidth curve extracted by the SPIDER by measurement. The curves is centered at 795.5nm rather than 773nm as it was in the earlier measurement. This is an improvement since Ti:S operates most efficiently at 800nm. The curve appears to be smoother than the curve in figure 1.41 because the SPIDER performs various filtering algorithms to extract the spectrum, which eliminated the noise caused by the scattering of the light into the spectrometer.

The spectral phase reconstructed by the SPIDER shows a significant third order contribution.

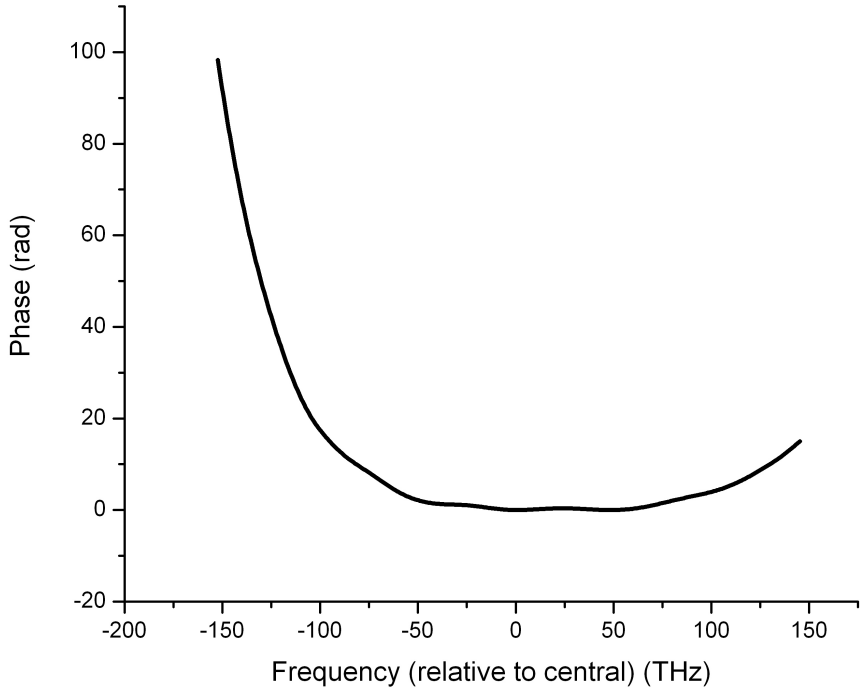

Fig. 1.43 Spectral phase of the pulse

The pulse shape is most significantly affected by fine phase modulation towards the central frequency of the pulse. These modulations are not very visible in this figure. Computing numerical derivatives of the spectral phase data revealed a value of 2376.85 fs^2 for the second order dispersion and a value of 12311.7 fs^3 for the third order dispersion in the pulse. The magnitude of these dispersion terms seems unusually high, however their magnitudes relative to each other seem reasonable based on residual dispersion values stated for similar oscillator designs [2].

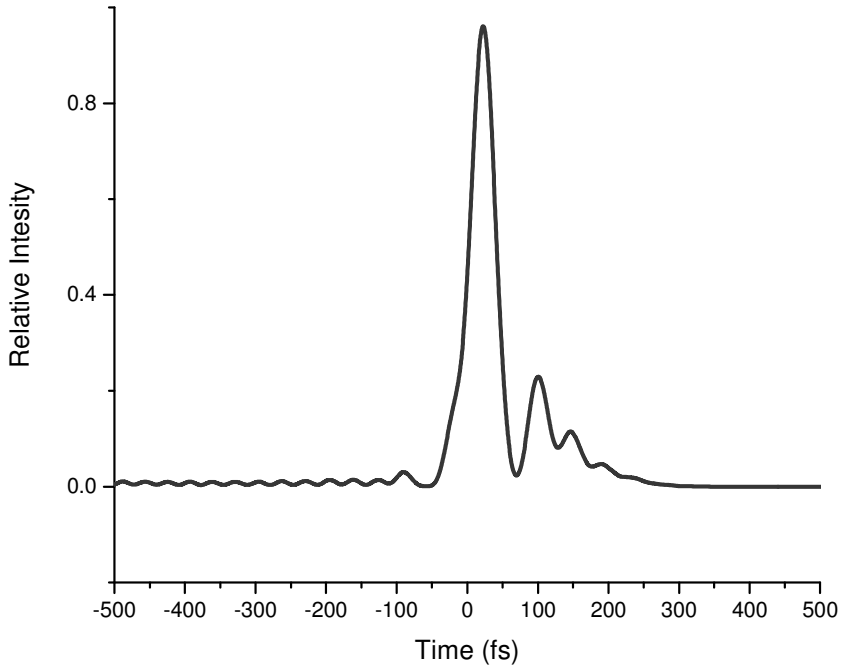

Fig 1.44 Reconstructed temporal profile of the pulse

The temporal envelope reconstruction shows the pulse to have a FWHM duration of 43fs. This is more than twice the transform limited duration for a 50nm pulse. The graph also shows several additional pulses following the main pulse, as well as some modulations preceding the pulse. The post-pulses can be explained as a result of the third order dispersion.

The unusually high magnitudes of the dispersion terms indicate that the SPIDER is may not be completely calibrated. A verification of the calibration involves reconstruction of pulses from an optimally tuned and well characterized laser oscillator as well as the addition of known amounts of dispersion to the pulses to ensure that the SPIDER characterizes this dispersion properly. A full calibration and characterization of the instrument had not been completed at the time of writing this report. Thus the spectral phase data are preliminary results. In addition the device that produces the measuremtns

signal for the SPIDER may not carry the entire bandwidth of this oscillator. Some upgrades to the SPDIER hardware may be needed to make more accurate measuremtns possible. This oscillator design is known to be capable of producing up to 100nm of bandwidth and pulses as short as 10fs [4]. Thus more tuning and alignment improvements will be needed for the completion of the oscillator.

2 Light Conversion with Nonlinear Optics

2.1 Non-Linear Polarization

Non-linear light conversion exploits effects that arise when a medium no longer responds completely linearly to an intense optical field.

A purely linear medium or vacuum responds proportionally to an incident optical field. In any transparent medium, light propagates by forward scattering from the atoms in the material. This scattering can be described with the dielectric polarization of a material. This is simply a measure of the average displacement of electrons from their parent atoms. The polarization can be found as a solution to a driven harmonic oscillator with the parameters of the atoms of the material and the driving force described by the incident light.

In a linear medium the polarization can be written as,

$$\mathbf{P}(t) = \chi^{(1)}\,\mathbf{E}(t) \quad \text{eq 2.11}$$

Where E(t) is the electric field describing the light incident on the material and $\chi^{(1)}$ is the first order susceptibility [6]. As shown in eq 2.1 the response is completely proportional to the incident light. This also implies that the response to several fields will be completely proportional to the incoming fields. This means that waves do not couple in a

linear medium, they may interfere at points of overlap, but they emerge from an intersection unaffected. In a nonlinear medium coupling of waves does occur. Non-linear media can be simulated by solving a harmonic oscillator with nonlinear restoring forces, in the presence of a very intense driving force. In this case the solution can be expanded in powers of the incoming field [6].

$$P(t) = \chi^{(1)} E(t) + \chi^{(2)} E(t)^2 + \chi^{(3)} E(t)^3 + \ldots + \chi^{(n)} E(t)^n \quad \textit{eq 2.12}$$

In the expansion the polarization has several terms at different powers of the electric field. In most media, the first order term dominates the polarization and higher order effects are insignificant at low intensities. The intensities produces by laser pulses are sufficient to drive nonlinear processes. The light conversion investigated in this experiment arises from the second order polarization response of a material. The electric field of light with two frequencies is described in complex notation as,

$$E(t) = E_a e^{i\omega_a t} + E_b e^{i\omega_b t} + c.c. \quad \textit{eq 2.13}$$

where ω_a and ω_b are the frequencies and E_a and E_b are the amplitudes of the fields (c.c. denotes the complex conjugate of the expression)[6]. The second order polarization caused by the light described in equation 2.13 is,

$$\begin{aligned} P^{(2)}(t) = {} & E_a^2 e^{i2\omega_a t} + E_b^2 e^{i2\omega_b t} \\ & + E_a E_b e^{i(\omega_a+\omega_b)t} + E_a E_b e^{i(\omega_a-\omega_b)t} \\ & + 2E_a^2 + 2E_b^2 + c.c. \end{aligned} \quad \textit{eq 2.14}$$

This response includes the doubling of each frequency ($2\omega_a$, $2\omega_b$), the sum of the frequencies ($\omega_a + \omega_b$), the difference of the frequencies ($\omega_a - \omega_b$) and constant electric fields ($2E_a^2$, $2E_a^2$) [6]. Higher order polarizations include triple and higher multiple frequencies as well as all possible combinations of sums and differences between the

incoming waves and the generated waves. The terms in the polarization expansion are also subject to quantum mechanical selection rules. A system with inversion symmetry (isotropic) such as a gas or liquid, cannot respond in even powers of the field. Second and all other even order processes can only be driven in a medium that does not have inversion symmetry (anisotropic) [6]. Crystals tend to be anisotropic. Thus the nonlinear conversion process requires a crystal with a significant nonlinear susceptibility.

2.2 Phase Matching

Since the conversion process takes place in a medium the waves will be subject to frequency dependant indices of refraction. This causes a change in the effective wavelength of the light in the medium. The result is a phase mismatch between waves generated at different points of the medium. This phase mismatch prevents the generated waves from adding up coherently in the crystal, thus making the generation inefficient or even impossible.

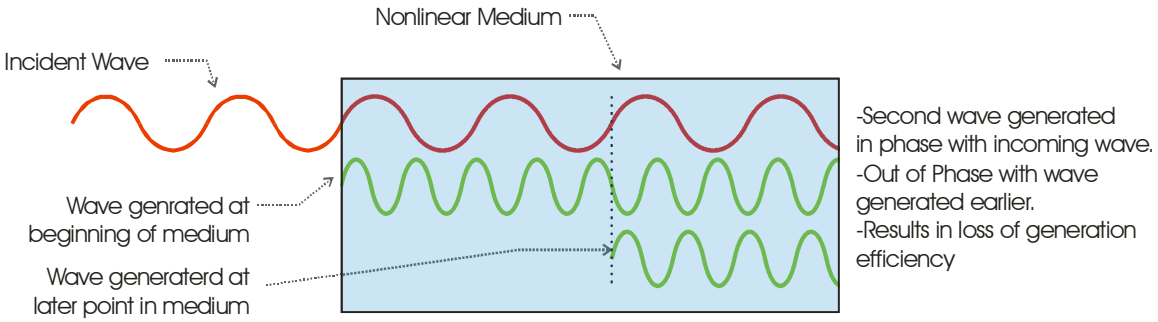

Fig 2.21 Illustration of phase mismatch in nonlinear conversion

In order to allow efficient nonlinear frequency conversion, the phases of the generated light waves must be matched throughout the medium. This can also be shown in terms of conservation of energy,

$$\omega_c = \omega_a + \omega_b \quad \textit{eq 2.21}$$

and momentum,

$$n_c \omega_c = n_a \omega_a + n_b \omega_b \quad \text{eq 2.22}$$

Equation 2.21 shows the photon energy relation for a conversion process where $\omega_{a,b,c}$ are the frequencies of the light fields interacting in the medium. This equation governs which frequencies have to be present for a conversion process. Equation 2.22 shows the conservation of momentum in the conversion process where $n_{a,b,c}$ are the respective indices of refraction for the interacting waves [6]. From this equation it is evident that the phase matched condition can be met if the indices are adjusted accordingly. To some extent this is possible by making use of birefringence in a crystalline material. Birefringence refers to the dependence of the index of a material on the relative angle between the light polarization and the crystal axis of the material. In processes that take place in birefringent materials the incoming light is polarized completely orthogonal to the crystal axis, this light is said to be on the ordinary axis. The generated light is then emitted in the plane of the crystal axis, this light is said to be polarized on the extraordinary axis. By changing the angle of the crystal, the angle between the generated wave polarization and crystal axis can be changed, thus adjusting the index experienced by the generated wave, without changing the index for the incoming wave.

The index $n_e[\Theta]$ experienced by the extraordinary wave can be expressed in terms of the angle Θ between the propagation vector of the light and the crystal axis,

$$n_e[\Theta] = \sqrt{\frac{1}{\frac{\text{Sin}^2[\Theta]}{\bar{n}_e^2} + \frac{\text{Cos}^2[\Theta]}{n_o^2}}} \quad \textit{eq 2.23}$$

where $\bar{n}_e$ and n_o are the wavelength dependant fundamental index values for the ordinary and extraordinary waves [6].

This method of phase matching is known as angle tuning. In some cases angle tuning may not completely correct phase mismatch in a conversion process. Some conversion processes are still impossible, despite angle tuning.

A more drastic approach to achieve phase matching, involves directly engineering a crystal tailored to the specific conversion process intended. One of these methods is known as periodic poling. A periodically poled crystal is grown to change the direction of its crystal axis at predefined intervals throughout the length of the crystal.

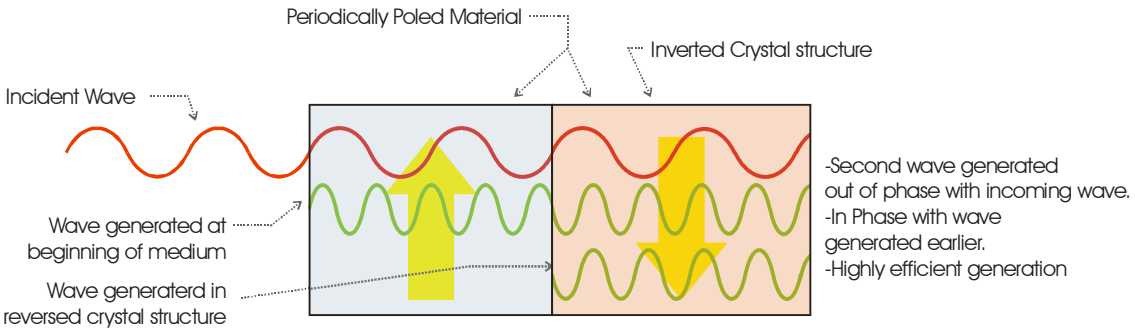

Fig. 2.22 Illustration of phase matching in a periodically poled material

The crystal axis reversal changes the sign of the nonlinearity thus causing a 180^{o} phase shift in the generated wave. As the generation process approaches the maximum efficiency allowed by the phase mismatch, the generation process moves through a reversal of the crystal structure which essentially resets the phase relationship between the waves. The periodically poled material provides for an extremely efficient conversion process that can be phase matched for wide variety of applications. The angle of the beams to the crystal axis is usually chosen at 90^{o} with extraordinarily polarized waves, for this application. This ensures that all waves experience the full fundamental extraordinary index of refraction. This allows for greater conversion bandwidth in frequency. Fine tuning of the conversion process can be accomplished by regulating the temperature of the crystal to thermally expand or contract the crystal structure. The

remaining limitations are the absorption profile and the damage threshold of the material. Advances in material engineering have recently made periodically poled materials available for research purposes. In order to use periodically poled materials the poling period must be calculated for the specific application.

2.3 Mid-Infrared generation from Ti:S Oscillator Pulses

The mid infrared ultra short pulses are to generated by difference frequency mixing of the spectral wings of an ultra short Ti:S Oscillator pulse in periodically poled lithium niobate (PPLN). For pulses centered at 800nm the required separation of the spectral components, to generate 4000nm pulses, is 158.43nm. This separation corresponds to spectral components centered at 720.79nm and 879.22nm.

Assuming that the oscillator operates at a full width half max bandwidth of approximately 100nm, with and average power of 400mW, the total energy of the 800nm pulses should be approximately 5nJ. The energy contained in each of the two spectral wing components would be 0.26nJ.

2.4 Preliminary Simulation Results:

Simulations of the conversion process were performed to estimate the resulting 4.0 micron pulse energy and to determine the best crystal length and focusing parameters. The simulations were conducted using an open source software package named SNLO, developed by Arlee Smith at Sandia National Labs. The software provides information on nonlinear material optical properties at different wavelengths as well as calculations for the proper poling period for crystals. SNLO also has the ability to compute the nonlinear

wave equation in the crystal to determine values such as pulse duration energy and spectral phase parameters of the generated light.

The poling period for the 4.0 micron process was calculated at 18.5 microns. The accepted bandwidth for the conversion process is estimated at 25-40nm for the 800nm light. The simulations were run by approximating the 800nm pulse components as two simultaneous 30fs pulses at 720.77nm and 879.22nm.

The values for phase and group velocity indices as well as group velocity dispersion in the material are as follows,

Wavelength (nm)	**Bandwidth (nm)**	**Duration (fs)**	**Phase velocity (v/c)**	**Group velocity (v/c)**	**GVD (*10^5 1/s)**
4000	784	30	2.0654	2.2468	5.228
879.22	37.8	30	2.1781	2.2586	-1.157
720.79	25.4	30	2.1975	2.3159	-1.471

Fig 2.41 Parameters for the three wave mixing process

The best performance was found at a beam diameter of 0.01mm, which can be achieved with a 25mm focal length lens, assuming the beam from the oscillator has a diameter of 5mm. The resulting fluence for the entire pulse at the focus is 4.41 mJ/cm^2 , which is much less than the damage fluence of 10 J/cm^2 for lithium niobate. The optimal crystal length was found running the simulations at various crystal lengths until the conversion appeared to be past the point of saturation.

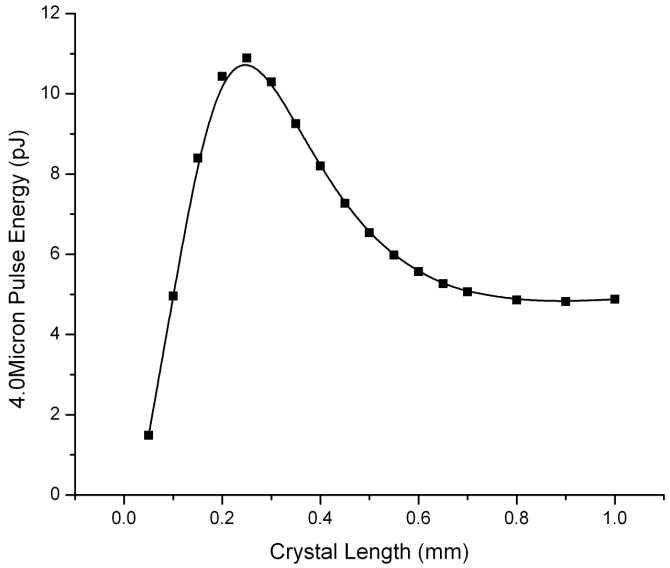

Fig 2.42 4.0 Micron pulse energy vs. crystal length

The optimal length was determined to be 0.25mm. At this length, the 4.0 micron pulse is generated with an energy of approximately 9.26pJ. In the time domain, the simulated pulse showed a duration of 40fs, which is about 30% longer than the minimum transform limited duration allowed by the bandwidth of the 800nm spectral wing components.

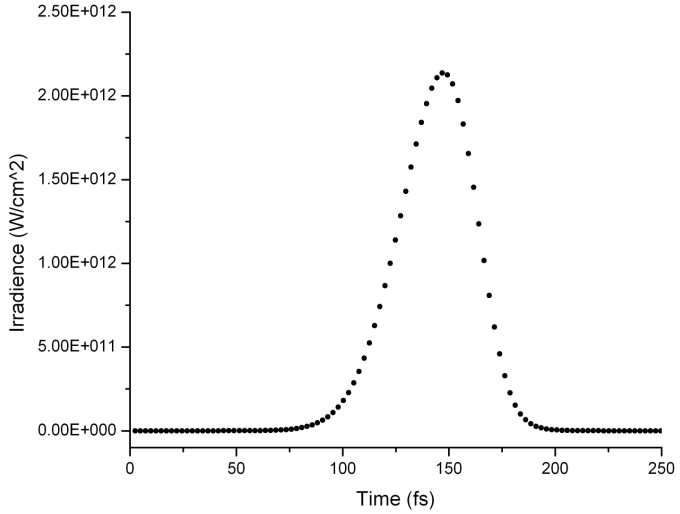

Fig 2.43 time profile of 4.0 micron pulse

Upon comparing the pulses spectra in frequency space it is evident that no bandwidth is lost in the conversion. Therefore the broadening must result from dispersion.

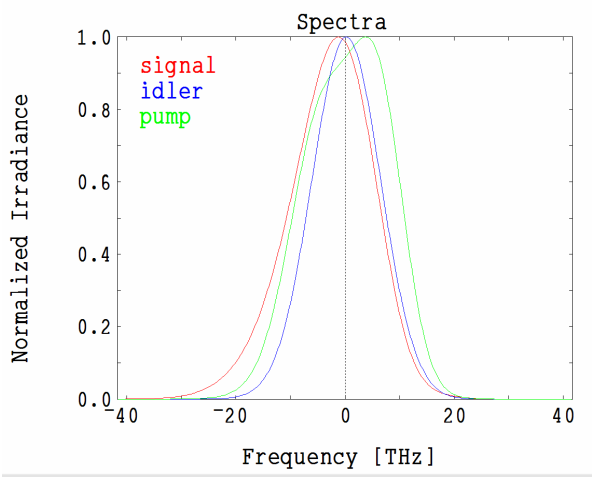

Fig 2.44 simulated relative frequency spectra of the pulses
Signal: 4.0 micron, Idler: 879.22nm, Pump: 720.79nm

The time dependant frequency shift shows the origin of the pulse broadening. Since 4.0 microns is in the vicinity of an absorption line in Lithium Niobate high GVD and TOD contributions should be expected.

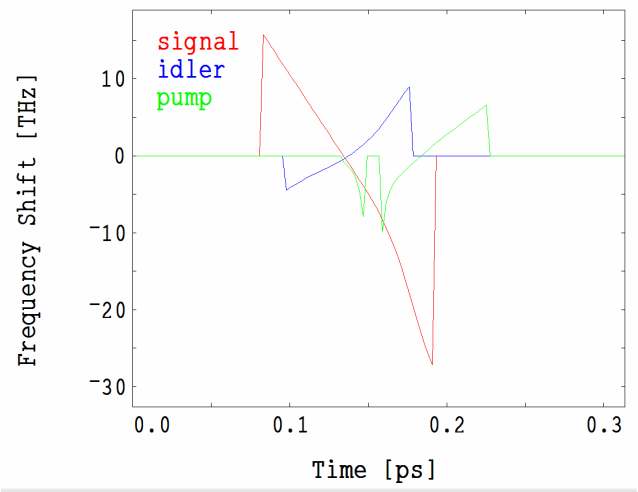

Fig 2.45 simulated frequency shift vs. time of the pulses
Signal: 4.0 micron, Idler: 879.22nm, Pump: 720.79nm

Figure 2.43 shows significant negative chirping of the 4.0 micron pulse. This negative chirp arises from anomalous dispersion due to the vicinity of 4000nm to an atomic

absorption near 5000nm in lithium niobate. As the wavelength approaches the absorption from shorter wavelengths the curvature of the index becomes negative, resulting in negative dispersion of pulses.

Based on these results some improvements could be made on the generation process. To provide more energy to the interaction the oscillator should be equipped with a tailored output coupler that emphasizes the spectral components that are needed to generate the mid-infrared pulse. The chirping of the mid-IR pulse suggests that a prism based delay stage should be implemented before the PPLN crystal to offset the anomalous chirping and to ensure that the spectral wing components are complete temporal overlap.

These simulations offer some insight into the energy, dimension and time scales of the conversion process. Further simulations are necessary to access the spatial properties of the conversion must be done. Once the spatial characteristic of the oscillator are more well defined, 2 dimensional conversion simulation can be made.

4. Conclusions:

Work on this Project so far has produced an operational modelocked titanium sapphire oscillator and preliminary computational studies of the nonlinear conversion process. The findings so far indicate that the 4.0 micron generation should be possible once the oscillator is brought to optimal performance specifications. Most of time spent so far was dedicated to determining the best design and mode of operation for the oscillator. The construction and alignment of the oscillator proved to be a very challenging task. However, building the laser produced another extremely useful tool for the laboratory as well as an incredible learning experience.

5. References:

1. I. Walmsley, L. Waxer, C.Dorrer, "The role of dispersion in ultrafast optics," Review of Scientific Instruments **17,**1 (2001)
2. G.D. Reid, K.Wynne, "Ultrafast Laser Technology and Spectroscopy," Encyclopedia of Analytical Chemistry pp.13644-13670, (2000)
3. A. Baltuska et al, "Efficient 50-THz-wide phase-stabilized chirped parametric amplification at 2.1μm" submission to CLEO-Europe, (2005)
4. M.Murnane et al, "Mode_locked Ti:Sapphire Laser Rev 1.7", Center for Ultrafast Optical Science, University of Michigan, (Feb. 1996)
5. M. Murnane et al, "Generation of 11 femtosecond pulses from a modelocked ti:sapphire laser," Optics Letters 18,977 (1993)
6. R. Boyd, "Nonlinear Optics, second edition", Academic Press, (2003)
7. E. Hecht, "Optics, fourth edition" Pearson Education, (2002)
8. C. Iaconis and A. Walmsley, "Spectral phase interferometry for direct electric-field reconstruction of ultrashort optical pulses" Optics Letters 23, 792-794 (1998)
9. I.N. Ross, "The prospects for ultrashort pulse duration and ultrahigh intensity using optical parametric chirped pulse amplifiers" Optics Communications 144, 125-133 (1997)